P1.13 IASI RADIANCE SIMULATIONS IN PREPARATION FOR NEAR REAL-TIME DATA DISTRIBUTION

Haibing Sun[2], C. Barnet[1], M. Goldberg[1],
T. King[2], and W. Wolf[2]

[1]NOAA/NESDIS/ORA
5200 Auth Road, Camp Springs, MD 20746 USA
[2]QSS Group Inc, Lanham, MD, USA

1. Introduction

Global atmospheric observing systems provide the basic data for Numerical Weather Prediction (NWP) forecasts and the means to monitor and assess climate change. The NOAA polar orbiting environmental satellite (POES) series has provided an operational environmental remote sensing capability since the early 1980s. The present POES program will evolve via collaboration with European Organization for the Exploitation of Meteorological Satellites (EUMETSAT) into the Initial Joint Polar system (IJPS) over the next 5 years. Ultimately, the current system will be augmented by a new generation of spacecraft and instruments in the National Polar Orbiting Environmental Satellite System (NPOESS). The cooperation between NOAA and EUMETSAT will provide increased spatial, spectral and temporal coverage for future atmospheric observing system.

IJPS consists of two independent, but fully coordinated, environmental polar-orbiting satellite systems. In IJPS, the National Environmental Satellite, Data, and Information Service (NESDIS) will continue to operate early morning and afternoon operational NOAA satellites, as well as generate, distribute, and archive an extensive suite of environmental products. EUMETSAT, working together with the European Space Agency (ESA), will develop the Meteorological Operational (MetOp) series of satellites to be flown in a polar orbit with a mid-morning (9:30 AM) equatorial crossing time. The NOAA and METOP satellites will each carry a set of common instruments along with additional instruments specific to each orbit and operating agency.

According to the IJPS agreement, NOAA and EUMETSAT are required to support each other's operational satellite through their respective ground segments for commanding, receiving telemetry and global data, monitoring their respective on-orbit status, and exchanging data between the two polar satellite systems. Through the use of these satellites, NOAA and EUMETSAT will support the generation of products and services for their respective user communities. IJPS will be a means for sharing polar satellite assets between the US and Europe.

* *Corresponding author address:* Haibing Sun, Room 810 WWB, NOAA/NESDIS, 5200 Auth Road, Camp Springs MD 20746; email: Haibing.sun@noaa.gov

In addition to providing data streams from all of the instruments on the NOAA satellites, NESDIS will also support four new MetOp instruments in order to enhance fulfillment of the NESDIS requirements. One of those four instruments (Infrared Atmospheric Sounding Interferometer (IASI) will be used initially by NESDIS and its users in a demonstration mode to complement the HIRS and AMSU-based soundings. Additional applications for the IASI may include sea surface temperature, clouds, Earth radiation budget, and land measurements. NESDIS will be responsible for the development of the real-time IASI data processing and distribution system to deliver the IASI data to NCEP and GMAO.

To support pre–launch preparation for the IASI near real-time processing and distribution system, an IASI on–orbit observation radiance simulation system is being developed within NOAA/NESDIS/ORA (Office of Research and Applications). The objective of this system is to: (1) provide simulated observation radiances that support cloud clearing algorithm development and testing, (2) provide a robust data distribution environment for development and testing of the IASI data sub-setting system, (3) enable a smooth transition of the IASI data processing system from the development environment to the operational environment, during both the integration and test phases of the transition.

The simulation system is designed to provide simulated IASI radiances to the users within an operational mode. The complete simulation processing will include: satellite orbit simulation, instrument observation footprint navigation simulation, surface property simulation, atmosphere profile simulation and radiative transfer simulation. In this paper, information about the MetOp satellite platform, IASI instrument, observation simulation methodology and details of the simulation system algorithms are presented.

1. MetOp Satellite

MetOp will be Europe's first polar-orbiting satellite dedicated to operational meteorology. It is a 3-axis stabilized satellite with the lateral side oriented in the flight direction. The MetOp polar orbit will be at an altitude from 800 to 850 km. The satellite orbit will not pass exactly over the geographic poles and is slightly slanted at a 98.7° inclination to the equator. This is done to benefit from variations in the gravitational pull on the satellite due to the Earth's shape (not completely round),

which causes the MetOp orbit to rotate at approximately 1° per day. From the MetOp point of view, the satellite orbit is in a constant position versus the sun, and the Earth will pass beneath the satellite ground track at 09:30 in the morning of every day and in all seasons, hence the term sun-synchronous orbit. The time to complete an orbit is about 101 minutes, this implies that MetOp will make a little more than 14 revolutions a day. During each orbit the Earth rotates approximately 25°, so that MetOp will observe a different portion of the Earth during each revolution. In sun-synchronous orbits the ground track repeats precisely after a constant integer number of orbits and days. The planned orbit for MetOp has a repeat cycle of 29 days and 412 orbits. During the operational life, the MetOp orbit will maintain the ground track within +/- 5 km and the local solar time within +/- 5 minutes.

2. Infrared Atmospheric Sounding Interferometer

IASI consists of a Fourier Transform Spectrometer based on a Michelson Interferometer, coupled to an integrated imaging system that allows the characterization of cloudiness inside the spectrometer field of view. The interferograms are processed by an on-board digital processing subsystem, which performs the inverse Fourier transforms and the radiometric calibration.

2.1 Spectral

The instrument provides spectra of high radiometric quality at 0.5 cm-1 resolution, from 645 to 2760 cm-1. The spectra are sampled at 0.25 cm-1 steps and result in 8461 "channels". Compared to existing operational satellite radiometers, this high spectral resolution instrument allows significantly improved accuracy and vertical resolution of retrieved temperature, humidity profiles and ozone profiles. The instrument is also designed for detection of additional trace gases and improved cloud characterization (Table 1.0).

Range, cm^{-1}	Primary application
650 - 770	Temperature sounding (CO_2-band)
770 - 980	Surface and cloud properties
1000 - 1070	Ozone sounding
1080 - 1150	Surface and cloud properties
1210 - 2100	Temperature and water vapor sounding CH_4, N_2O et SO_2 (column amounts)
2100 - 2150	CO (column amount)
2150 - 2250	Temperature sounding (CO_2 band)
2350 - 2420	Temperature sounding (CO_2 band)
2420 - 2700	Surface and cloud properties
2700 - 2760	CH_4 (column amount)

Table 1.0 IASI spectral ranges and primary applications

2.2 Scan & Sampling

The instrument samples 30 Earth views along an across-track scan, over a total swath width of about 2200 km. The overall swath is ± 48.3° with respect to the nadir direction, corresponding to 30 mirror positions. The IASI interferometer field of regard (FOR) is square, seen under an angle of 3.33 x 3.33° (Figure 1). Information matrix of 2 x 2 circular pixels seen under an angle of 1.25°.

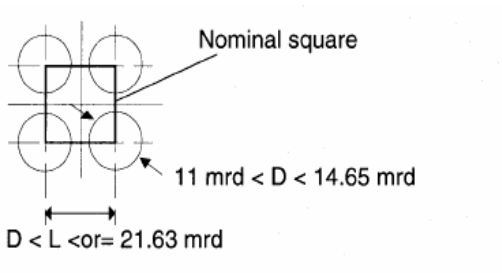

Figure 1.0 IASI Element Field Of Regard

The distance between two Earth FORs is about 50 km at nadir. Within each FOR, the sub-pixels each have a maximum diameter of 12 km at nadir. The scan duration (8 seconds) and the horizontal spacing of the full Earth FORs are identical to those of the AMSU_A instrument so as to facilitate synergistic use of the two instruments. Furthermore, in order to achieve registration with AVHRR, the instrument will include an integrated imager that samples the IASI sounder pixels with a kilometric spatial resolution.

2.3 Calibration

IASI calibration relies on the measurement of cold and hot reference targets once every scan line. The measurements are done in the same instrument configuration as the earth scenes.

3. Observation radiance simulation methodology

The radiance at the top of the atmosphere measured by a satellite instrument at a spectral interval ν and zenith angle θ can be broken into components from the surface emission, I_s, atmospheric column emission upward, I_c, reflected down-welling atmosphere emission, I_d, and reflected solar radiance, I_{sun}.

$$I(\nu, \theta) = I_s(\nu, \theta) + I_c(\nu, \theta) + I_d(\nu, \theta) + I_{sun}(\nu, \theta, \theta_{sun}) \quad (1.0)$$

in which θ_{sun} is solar zenith angle.
The surface emission can be written as:

$$I_s(\nu, \theta) = \varepsilon_s(\nu,\theta)\, B(\nu,T_s) \exp(\tau(\nu, \theta, P_s)) \quad (2.0)$$

where ε_s is the spectral surface emissivity $B(T_s)$ is the Planck function and, Ts is the surface temperature. τ (ν, θ, Ps) is the surface to space transmittance from the surface, at pressure *Ps* to the instrument.

The atmospheric transmittance is related to the absorption of radiation by all the gases within the

atmosphere. The absorption of each gas, with index *i*, is given by an absorption coefficient, k*i*(*v, z*). The absorption coefficients are strongly dependent on the composition of the atmosphere, *a*(*i, z*), temperature, *T* (*p*(*z*)), and pressure, *p*(*z*), along the path. The transmittance is a vertical integral of the absorption coefficients. Transmittance from atmosphere with pressure P to instrument can be written as:

$$\tau_V(P,\theta) = e^{\int_{\infty}^{z=z(p)} -\sum_i k_V^i(T(z),z).\sec(\theta).d\,z} \quad (3.0)$$

Transmittance from atmosphere with pressure P to surface can be written as:

$$\tau_{s-V}(P,\theta) = e^{\int_{z=z(p)}^{z=z(p_s)} -\sum_i k_V^i(T(z),z).\sec(\theta).d\,z} \quad (4.0)$$

The atmospheric emission for a plane, parallel atmosphere in a local thermodynamic equilibrium is given by:

$$I_c(v,\theta) = \int_{z=z(p_s)}^{\infty} B_V(T(z)).\frac{\partial \tau_v(p,\theta)}{\partial z}.d_z \quad (5.0)$$

The reflected atmospheric down-welling radiance I_d originate in the atmosphere above the surface and is reflected by the surface .The radiant energy reflected into the solid angle comes from all direction above the surface. I_d can be written as:

$$I_d(v,\theta) = \tau_v(p_s,\theta) \int_{z=\infty}^{z=p_s} \int_{\theta'=0}^{\theta'=2\pi\pi/2} \int_{\varphi=0} B_V(T(z,\theta',\varphi)) \frac{\partial \tau_{s-v}(p,\theta')}{\partial z} \rho(\theta',\theta).\sin(\theta')\cos(\theta')\, d_{\theta'} d_{\varphi} . d_z \quad (6.0)$$

The reflected solar term is given by the solar radiance outside the Earth's atmosphere, S(*v*), and the reflectivity of the surface, ρ(v, θ, θ_{sun}).

$$I_{sun}(v,\theta,\theta_{sun}) = \mathrm{S(v)}\cos(\theta_{sun})\exp(-\tau_{s-v}(p,\theta_{sun}))\, p_v(v,\theta,\theta_{sun})\exp(-\tau_v(p,\theta)) \quad (7.0)$$

Where θ_{sun} is the sun zenith angle and θ is the observation zenith angle.

A channel radiance I_n is a convolution of a channel response function φ_v and the monochromatic radiance I_v.

$$I_n(v,\theta) = \int I_V . \varphi_V d_V \quad (8.0)$$

The data required in the simulation calculation include: zenith angle and solar zenith angle at each of IASI pixels; surface temperature Ts, pressure Ps emissivity/reflectivity, atmosphere composition and temperature profile that is used for atmosphere transmittance calculation. A radiative transfer model is required to calculate the observation radiance. This IASI observation system include: an orbit simulation module providing satellite orbital ephemeris and attitude data; a geolocation simulation module providing instrument pointing data, field of view location data; a surface simulation module to simulate the surface properties, including emissivity and reflectivity; an atmospheric simulation model to provide atmospheric data, and a radiance forward module to calculate the observation radiances.

The architecture of the IASI observation radiance is given in figure 2.0.

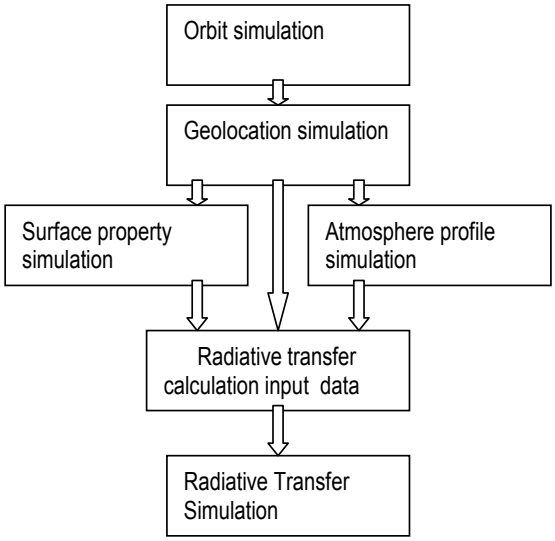

Figure 2.0 The Architecture of the IASI Observation Simulation System.

4. Observation simulation of the IASI data

4.1 MetOp orbit simulation

Orbital simulations provide satellite ephemeris attitude data for the navigation simulation processing. An orbit simulator was developed based upon the orbit simulator in SDP Toolkit, which is a Software package developed by Raytheon for ECS system. In the orbit simulator, the orbit is defined by six keplerian elements at epoch:

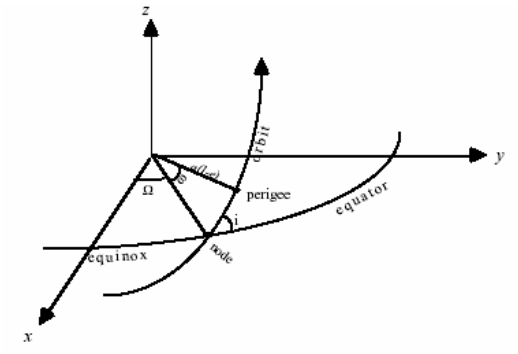

Figure 3.0 Keplerian element

α - true anomaly (instaneous angle from satellite to perigee)
ω - argument of perigee
Ω - longitude of node
a - semi major axis
e - eccentricity
i - inclination

4.2 *Geolocation Simulation*

The function of the geolocation simulations include:

1: Computing geodetic longitude and latitude of the Earth located center of each field of view (FOV). Longitude and latitude data are used in surface property simulation.

2: Computing the line of sight (LOS) slant angle Γ of the located measurement.

3: Computing land fraction, surface elevation with each footprint.

4: Computing solar/moon position vector.

Footprint position is evaluated from the IASI detector pointing vector relative to the instrument coordinate system, spacecraft ephemeris and attitude data and the time of the measurement. Time is nominally reported in seconds of secTAI93 (seconds Temps Atomique International, 1993 epoch). The land fraction, surface elevation and their errors are integrated quantities evaluated by sampling a digital elevation model (DEM) within the IASI footprint.

The following are the simulation procedures:

1: Transform the spacecraft position vector and the detector pointing vector into an Earth fixed coordinate system.

2: Define the equation of the line passing through the spacecraft position and parallel to the detector pointing vector, and combined with the Earth ellipsoid equation to form a system of equations.

3: The solution of the system determines the points of intersection between the line and the ellipsoid.

4: Computes the zenith and the azimuth of a vector at the look point. Computes the solar zenith and the solar azimuth at the look point.

5: Samples a DEM over the IASI footprint to get land fraction and surface elevation.

The functions for coordinate system conversion, celestial body position and digital elevation model are from the SDP Toolkit.

The IASI instrument is equipped with a hollow cube-corner retro-reflectors in place of the classical flat mirrors. In order to prevent spectrum contamination due to variation of instantaneous field of view content, it is required to stationarize instantaneous field of view on ground during the time necessary to one interferogram acquisition. To simplify IASI scanning simulation, a flat mirror reflector model is used to simulate this “step and stare” sampling scheme. The simulated sub-pixels keeps its center stationary during interferogram acquisition time (about 151 ms).

4.3 Surface Properties Simulation

The surface properties relating to the observation radiance calculation include skin temperature, surface pressure, topography, infrared emissivity and reflectivity. Land fraction and topography can be obtained for the geolocation simulation module by sampling DEM. Skin temperature and surface pressure are obtained from the NCEP GCM data at the FOV locations. The emissivity and reflectivity are obtained by linear interpolation in frequency with the emissivity and reflectivity at the frequency hinge points, which are the frequencies at which the properties are specified. The infrared surface emissivity and reflectivity at the hinge points are calculated based on surface material properties within each footprint. Currently, seven surface materials are used. These materials include sea water, one type of ice, two types of soils and three types of vegetation. All materials are assumed to be Lambertian reflectors in the infrared. The contribution of each material is determined by land fraction, the amount of vegetation and the types of vegetation defined by the International Geosphere Biosphere Program (IGBP) land use surface classification, and three or fewer random uniform normalized varieties. The IGBP land use class of each footprint is determined from a digital IGBP land use map and the location data from the geolocation simulation. Vegetation and water amounts are determined from AVHRR NDVI imagery and the sampled DEM (USGS) and the FOV position.

The emissivity for the ices and vegetation are interpolated from emissivities produced by the CERES group (Wilber, et al. 1999). Emissivities of the two soil types were obtained from the Infrared Handbook (Wolfe and Zissis, 1978) and a simplified model. Ocean emissivity is determined by a functional fit to the

tabulated values of an upgraded Masuda model (Masuda et. al., 1988). The upgraded model use sea surface emissivities derived via the Wu and Smith (Wu et al 1997) methodology as described in van Delst and Wu (van et al 2000)

4.4 Atmosphere Simulation

Atmospheric radiance transmittances are strongly dependent upon the composition of the atmosphere, the temperature, and the pressure along the path. The transmittance is a vertical integration of the absorption coefficients. In the atmospheric simulation module, the temperature profile and volume-mixing ratio profiles for the most radiatively active molecules (H2O, O3, CO2, CO, and CH4) are provided.

The ECMWF forecast data, the UARS climatology and the Harvard tropospheric ozone climatology are used for the atmosphere profile data. The ECMWF forecast is provided by the European Centre for Medium-Range Weather Forecasts (ECMWF). In the ECMWF data, temperature, humidity and liquid water profiles are provided. In present test period, an ECMWF nature run data is used in the simulation. The description and evaluation of the nature run is given in Becker et al. (1996).

The UARS climatology data consists of monthly and zonally averaged means and variances of temperature and eighteen other species including water vapor, ozone, methane and carbon monoxide. The UARS profiles are provided at 31 pressure levels. The Harvard tropospheric ozone climatology contains monthly tropospheric ozone values in 13 pressure levels.

4.4.1 Air Temperature

The air temperature profile is obtained from the ECMWF nature run and the UARS temperature climatology. The two profiles are combined with a tie point at the top of the nature run forecast pressure levels.

4.4.2 Water Vapor

The ECWMF data contains profiles of relative humidity. If data is missed at the up level atmosphere, the profiles can be extrapolated upward using a power law.

$$X_{H_2O}(p) = X_{H_2O}(p^T)(p / p^T)^3 \qquad (9.0)$$

where p^T is the pressure at the top of the ECMWF levels.

4.4.3 Ozone

Ozone data is provided by the UARS climatology for the upper stratosphere and mesosphere. The Harvard climatology provides a better estimate of the troposphere. The two data sources are combined at 100 hPa to obtain the ozone profile used in radiance simulation.

4.4.4 Other constituents

The atmosphere methane profile is provided by Gunson *et. al.*, (1990). Atmospheric carbon monoxide profiles are taken from the U.S. standard atmosphere.

In atmosphere carbon dioxide profile specification, a model developed at the Jet Propulsion Laboratory is used (Fishbein et al, 2003). This model is based on measurements of CO_2 at ground stations and a realistic representation of meridional and vertical transport. In the model, a positive secular trend, seasonal variability and a surface source whose rate is slow compared to transport are included.

4.4.5 Clouds

In the IASI radiance simulation, the required cloud parameters are cloud top and bottom pressures, cloud liquid water, cloud fraction, cloud emissivity and cloud reflectivity. The cloud liquid water and cloud fraction on each sigma level are provided by the ECMWF nature run. The clouds are stratified into three groups, high, middle and low defined by cloud bottom pressures above 300 hPa, between 500 hPa to 300 hPa, and below 500 hPa, respectively. All clouds are assumed to be opaque and Lambertian reflectors.

4.5 Instrument forward models

Instrument forward models are required in order to generate simulated observations that would have the same characteristics as real observations. The fast forward model was developed based on the pre-launch spectral response functions was provided by Larabee Strow at UMBC (Strow et. al 2003).

4.6 Simulation Outputs

The simulated IASI radiances are produced in BUFR (Binary Universal form for the Representation of meteorological data) format. The format of the BUFR files will be a combined effort between NOAA/NESDIS/ORA and the representatives from the global NWP centers.

5. Summary

The purpose of this work is to provide simulated IASI observation radiance for the IASI near real-time data distribution system developed in NOAA/NESDIS/ORA. In this paper, the procedure of the simulation and the data sets used were described

6. REFERENCES

Atlas, R., E. Kalnay and M. Halem, 1985a: The impact of satellite temperature sounding and wind data on numerical weather prediction.
Optical Engineering., 24, 341-346.

Atlas, R., E. Kalnay, J. Susskind, W. E. Baker and M. Halem, 1985b: Simulation studies of the impact of future observing systems on weather prediction. *Proc. Seventh Conf. On NWP*. 145-151.

Becker, B. D., H. Roquet, and A. Stofflen 1996: A simulated future atmospheric observation database including ATOVS, ASCAT, and DWL. *BAMS*, 10, 2279-2294.

D.Barnet Theoretical Background for the AIRS Diagnostic Retrieval Code(ADRC), 2003

E.Fishbein,C.B.Farmer,S.L.Granger David T. Gregorich. Michael R.Gunson, Scott E.Hannon ,Mark D.hofstadter ,Sung-Yung Lee, S.S Leroy, L.Larabee Strow. 2003: Formulation and Validation of Simulation Data for the Atmospheric Infrared Sounder. *IEEE* vol 41, No.2.

Gunson M. R., C. B. Farmer, R. H. Norton, R. Zander, C. P. Rinsland, J. H. Shaw, B. C. Gao, 1990: Measurements of CH, NO, CO, HO, and O in the middle atmosphere by the Atmospheric Trace Molecule Spectroscopy experiment on SPACELAB-3, *J Geophys. Res*., 95, 13,867–13,882.

L.Larrabee Strow, Scott E. Hannon, Sergio De Souza-Machado, Hpward E.Motteler, Member, IEEE, and David Tobin ,2003 An Ovew of the AIRS Radiative Transfer Model. *IEEE* vol 41, No.2.

McMillin, L. M., L.J. Crone, and T.J. Kleespies, 1995: Atmospheric Transmittance of an Absorbing Gas 5. Improvements to the OPTRAN Approach, *Applied Optics*, vol34 no36.

Masuda, K., T. Takashima, and Y. Takayama, 1988: Emissivity of Pure and Sea Waters for the Model Sea Surface in the Infrared Window Region, *Remote Sensing of the Environ*., 24, 313–329.

Noerdlinger, P. D., 1995: Theoretical Basis of the SDP Toolkit Geolocation Package for the ECS Project, *Hughes Appl. Info. Sys. Tech. Pap. 445-TP-002-002*, 201pp., May 1995.

Morse, P., J. Bates and C. Miller, 1999: "Development and Test of the Atmospheric Infrared Sounder (AIRS)", *Proceedings of SPIE, Infrared Spaceborne Remote Sensing VII, Volume: 3759*

Salisbury, J. W. and D. M. D'Aria, 1992: Emissivity of terrestrial materials in the 8-14 m atmospheric window*, Remote Sensing of the Environ*., 42, 157–165.

Strow, L. L., H. E. Motteler, R. G. Benson, S. E. Hannon, and S. De Souza-Machado, 1998: Fast computation of monochromatic infrared atmospheric transmittances using compressed lookup tables .*J. Quant. Spectrosc. Radiat. Transfer,* 59, 481-493.

USGS, 1987. Digital Elevation Models, Data Users Guide 5, US Department of the Interior, USGS, Reston, VA.

van Delst, P.F.W. and Wu, X. A high resolution infrared sea surface emissivity database for satellite applications. *Technical Proceedings of The Eleventh International ATOVS Study Conference*, Budapest, Hungary 20-26 September 2000, 407-411.

Wolfe, W. L. and G. J. Zissis, 1978: The Infrared Handbook, Office of Naval Research, Dept. of the Navy, Washington, DC, 1978.

Wilber, C. W., D. P. Kratz, S. K. Gupta, 1999: Surface emissivity maps for use in satellite retrievals of long wave radiation, *NASA Tech Rep Rep. Tp - 19999209362,* 27pp.

Wu, X. and Smith W.L. 1997. Emissivity of rough sea surface for 8-13μm: modeling and verification. *Appl. Opt*., 36, 2609-2619.